Nikolaevskiy equation with dispersion

Eman Simbawa,* Paul C. Matthews,† and Stephen M. Cox‡
School of Mathematical Sciences, University of Nottingham, Nottingham NG7 2RD, United Kingdom
(Received 30 June 2009; revised manuscript received 12 March 2010; published 26 March 2010)

The Nikolaevskiy equation was originally proposed as a model for seismic waves and is also a model for a wide variety of systems incorporating a neutral "Goldstone" mode, including electroconvection and reaction-diffusion systems. It is known to exhibit chaotic dynamics at the onset of pattern formation, at least when the dispersive terms in the equation are suppressed, as is commonly the practice in previous analyses. In this paper, the effects of reinstating the dispersive terms are examined. It is shown that such terms can stabilize some of the spatially periodic traveling waves; this allows us to study the loss of stability and transition to chaos of the waves. The secondary stability diagram ("Busse balloon") for the traveling waves can be remarkably complicated.

DOI: 10.1103/PhysRevE.81.036220 PACS number(s): 89.75.Kd, 47.54.−r, 82.40.Ck

I. INTRODUCTION

In 1989, Nikolaevskiy [1] derived a model for longitudinal seismic waves, in the form of a one-dimensional partial differential equation (PDE) for a displacement velocity. Although Nikolaevskiy's equation included dispersive terms, most subsequent analysis has treated a simplified version of the PDE, in which these terms are omitted. This reduced form is now generally known as the *Nikolaevskiy equation*, which may be written in the form

$$\frac{\partial u}{\partial t} = -\frac{\partial^2}{\partial x^2}\left[r - \left(1 + \frac{\partial^2}{\partial x^2}\right)^2\right]u - u\frac{\partial u}{\partial x}, \tag{1}$$

where r is a control parameter. Equation (1) has been proposed as a model for several other physical systems, including phase instabilities in reaction-diffusion equations [2], electroconvection [3], and transverse instabilities of fronts [4]. More generally, Eq. (1) can be regarded as a simple model of a pattern-forming system with an instability at finite wave number and a neutral "Goldstone" mode arising from symmetry [3,5].

The uniform state $u \equiv 0$ of Eq. (1) becomes unstable at $r=0$ to spatially periodic "roll" solutions, with wave numbers around $k=1$. However, these, in turn, are themselves all unstable at onset in sufficiently large domains [3]; this unusual instability arises from the neutral mode at wave number $k=0$. In fact, numerical simulations show that the Nikolaevskiy equation exhibits spatiotemporal chaos at onset [5,6]. The scalings associated with this chaotic regime are unusual in pattern-forming systems [5,7], and this interesting feature of the equation has stimulated significant investigation [8].

Although in some applications (such as the instability of fronts [4]) the omission of dispersive terms is justified on symmetry grounds, this is not the case in the original context of a model for seismic waves [1].

Earlier work that *has* considered the effects of dispersion includes the paper of Malomed [9], who reinstated one dispersive term in the Nikolaevskiy equation and analyzed the secondary stability of traveling-wave solutions by means of coupled Ginzburg-Landau-type equations for the amplitude of the traveling waves and a large-scale mode. His results showed that dispersion could stabilize waves; however, his derivation was not entirely asymptotically self-consistent [3]. Kudryashov and Migita [10] showed, on the basis of numerical simulations, that traveling waves can be stabilized by the presence of dispersive terms in the Nikolaevskiy equation. It is also known that in the related Kuramoto-Sivashinsky equation, the introduction of a dispersive term can stabilize periodic traveling waves [11].

Our aim in this paper is to provide a systematic examination of the effects of dispersion. By varying the parameters corresponding to dispersion, we can find when dispersion stabilizes traveling waves and investigate how the chaotic state in the nondispersive equation arises as the dispersion is reduced.

In the following section we give the form of the equation and the traveling waves under consideration. Computational results on the stability of these waves are given in Sec. III. The stability analysis of the waves is complicated and depends on the magnitude of the dispersion terms; three different scalings are considered in Secs. IV–VI. Section VII illustrates some numerical simulations of the Nikolaevskiy equation with dispersion, and our conclusions are summarized in Sec. VIII.

II. NIKOLAEVSKIY EQUATION WITH DISPERSION

We examine the Nikolaevskiy equation with dispersion in the form

$$\frac{\partial u}{\partial t} = -\frac{\partial^2}{\partial x^2}\left[r - \left(1 + \frac{\partial^2}{\partial x^2}\right)^2\right]u - u\frac{\partial u}{\partial x} + \alpha\frac{\partial^3 u}{\partial x^3} + \beta\frac{\partial^5 u}{\partial x^5}, \tag{2}$$

where α and β are the dispersion coefficients. This equation is thus the one originally proposed by Nikolaevskiy [1] (and later examined in [9,10]), with all spatial derivatives up to the sixth appearing on the right-hand side. In the numerical

*pmxes3@nottingham.ac.uk
†paul.matthews@nottingham.ac.uk
‡stephen.cox@nottingham.ac.uk

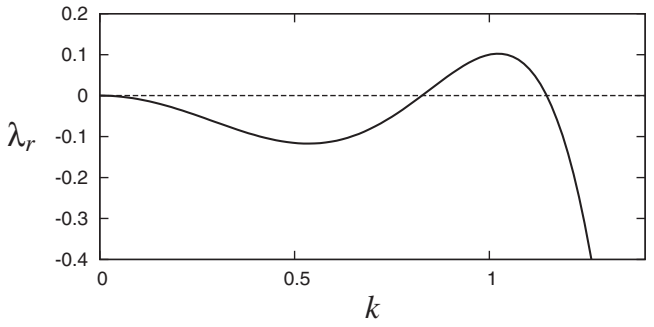

FIG. 1. Plot of λ_r for the case $r=0.1$: note the linearly growing modes with wave number around $k_c=1$ and the weakly damped large-scale modes close to $k=0$.

simulations presented in Sec. VII, we shall impose the periodic boundary condition

$$u(x+D,t)=u(x,t) \tag{3}$$

for some domain length D.

Before proceeding, we note that Eq. (2) has the same Galilean symmetry ($x\mapsto x+Vt$, $u\mapsto u+V$) as nondispersive Eq. (1). Moreover, in view of the Galilean symmetry and the observation that, when boundary condition (3) is imposed,

$$\frac{d}{dt}\int_0^D u(x,t)dx=0,$$

the spatial average of u may be set as zero (by transforming to a moving frame of reference if necessary). The reflection symmetry ($x\mapsto -x$, $u\mapsto -u$) of Eq. (1) is broken by the presence of the dispersive terms. However, there is a symmetry $x\mapsto -x$, $u\mapsto -u$, $\alpha\mapsto -\alpha$, and $\beta\mapsto -\beta$; as a consequence of this symmetry we need consider only the case $\beta\geq 0$.

Linearization around the steady state $u\equiv 0$ yields the dispersion relation

$$\lambda=k^2[r-(k^2-1)^2]+ik^3(k^2\beta-\alpha)$$

for Fourier modes proportional to $e^{ikx+\lambda t}$. Thus in general these perturbations take the form of traveling waves, with phase speed

$$c_p=-\frac{\lambda_i}{k}=k^2(\alpha-k^2\beta) \tag{4}$$

and group velocity

$$c_g=-\frac{\partial\lambda_i}{\partial k}=k^2(3\alpha-5\beta k^2). \tag{5}$$

The real part of the growth rate, λ_r, is plotted in Fig. 1, for r just above the threshold value $r_c=0$ for the onset of instability. This figure shows that there exists a band around the critical wave number $k_c=1$ of linearly growing modes, and a neutral mode at $k=0$ (the so-called "Goldstone mode"), which significantly affects the nonlinear dynamics of Eq. (2).

Just beyond the onset of instability of the zero solution, it is straightforward to carry out a weakly nonlinear analysis of Eq. (2), with

$$r=\epsilon^2 r_2. \tag{6}$$

This analysis reveals that there are traveling-wave solutions of the form

$$u\sim \epsilon a_0 e^{ik(x-st)}+\text{c.c.}, \tag{7}$$

where the wave number $k=1+\epsilon q$. The amplitude turns out to be given by

$$a_0=6(r_2-4q^2)^{1/2}\left(1+\tfrac{1}{36}(\alpha-5\beta)^2\right)^{1/2} \tag{8}$$

and the speed of the wave is

$$s=c_p-\tfrac{1}{6}\epsilon^2(r_2-4q^2)(\alpha-5\beta)+o(\epsilon^2), \tag{9}$$

where c_p is given by Eq. (4) and the second contribution to s reflects (weakly) nonlinear effects. So, regardless of the values of the dispersion parameters α and β, such spatially periodic solutions exist for $r_2>4q^2$. We now turn to the question of the secondary stability of these solutions.

III. SECONDARY STABILITY OF TRAVELING WAVES: NUMERICAL RESULTS

In this section we first outline a numerical method for the calculation of the nonlinear traveling waves and their secondary stability, and then give the results of these computations, showing the stability boundaries of traveling waves.

A. Numerical method for calculating secondary stability

To calculate the secondary stability of a traveling-wave solution for given values of the parameters, we first find the traveling-wave solution $\bar{u}(x,t)=f(z)$, where $z=x-ct$. Here, c is the nonlinear wave speed, which in general is not exactly equal to the linear wave speed c_p of Eq. (4). We approximate the solution numerically using the truncated Fourier series

$$f(z)=\sum_{-N/2+1}^{N/2}\bar{u}_n e^{inkz}.$$

Substitution in Eq. (2) (and calculation of the nonlinear term pseudospectrally) yields a system of nonlinear equations (solved in MATLAB) for the Fourier coefficients of $f(z)$, together with c, which is determined from

$$c\int_0^D (f')^2dz=\alpha\int_0^D (f'')^2dz-\beta\int_0^D (f''')^2dz+\int_0^D f(f')^2dz, \tag{10}$$

where $D=2\pi/k$ is the length of the domain and k is the wave number of the solution under consideration. Expression (10) follows from multiplying Eq. (2) by $f'(z)$ and integrating over the domain, using integration by parts multiple times. To compensate for the additional unknown c, we have an additional equation from the fact that we may choose the phase of the wave, for example, by specifying that $\bar{u}_1$ is real.

After calculating the solution, we construct the eigenvalue problem for perturbations. If we suppose that $u(x,t)=f(z)+\tilde{u}(x,t)$, then substitution in Eq. (2) yields the linearized perturbation equation

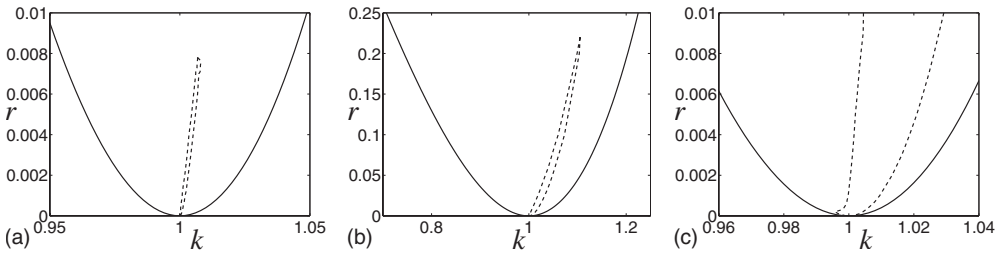

FIG. 2. The secondary stability regions of traveling waves of Eq. (2), calculated numerically for (a) $\alpha=1/2$, (b) $\alpha=2$, and (c) $\alpha=5$, all for $\beta=0$. Shown are the marginal curve $r=(1-k^2)^2$ (solid line) and the secondary stability boundary of the traveling waves (dashed line), with stability between the dashed lines.

$$\frac{\partial \tilde{u}}{\partial t} = -\frac{\partial^2}{\partial x^2}\left[r - \left(1+\frac{\partial^2}{\partial x^2}\right)^2\right]\tilde{u} + \alpha\frac{\partial^3 \tilde{u}}{\partial x^3} + \beta\frac{\partial^5 \tilde{u}}{\partial x^5} - f(z)\frac{\partial \tilde{u}}{\partial x} - \tilde{u}f'(z). \tag{11}$$

We take

$$\tilde{u} = e^{\sigma t + ipz}\sum_{-N/2+1}^{N/2} v_n e^{inkz},$$

where all possible eigenfunctions may be captured by limiting consideration to $-k/2 \le p \le k/2$. The resulting eigenvalue equations to determine the growth rate σ are then

$$(\sigma - icK_n)v_n = \mathcal{L}v_n - \sum_{-N/2+1}^{N/2} iK_m v_m \bar{u}_{n-m} - \sum_{-N/2+1}^{N/2} imkv_{n-m}\bar{u}_m,$$

where $\mathcal{L}=K_n^2(r-(1-K_n^2)^2)-i\alpha K_n^3+i\beta K_n^5$ and $K_n=p+nk$. The eigenvalues of this system are computed numerically. By examining the largest real part of all eigenvalues σ for a large sample of values of p in the relevant interval, we determine whether the original traveling waves are stable or unstable. In Sec. III B we provide some stability diagrams based on the above method.

In determining our results, we have been careful to check that: adequate samples in p are taken (too few, particularly for small values of p, can lead one to miss certain small regions of instability); adequate Fourier modes are taken in determining both the original solution and the perturbations; adequate samples are taken in parameter space to determine all regions of stable rolls. Typically, 300 values of p are used, with $N=16$.

B. Results

Now we present the secondary stability diagrams. The first case considered here is setting $\beta=0$ and varying α (see Fig. 2). When α is small ($\alpha=1/2$), there is a very small region of stable waves in the (k,r) plane. The stable region is a thin strip, confined to small values of r; in this case, for $r>0.0078$ all rolls are unstable.

For larger α this strip of stable waves is longer and wider; for example, at $\alpha=2$ there are some stable rolls up to $r \approx 0.22$, and at $\alpha=5$ the stability region extends at least as far as $r=0.9$. Furthermore, it is apparent for $\alpha=5$ that a symmetrical Eckhaus-like stability region is present for very small values of r (from the numerical results themselves, it seems to be present in all three cases but is visible only in the last plot of Fig. 2). The shrinkage of the region of stable traveling waves for small α is consistent with there being no stable rolls at all in the nondispersive case.

While an exhaustive examination of the secondary stability diagrams across (α,β) parameter space is infeasible, it is worthy of note that these diagrams may be extremely complicated. A good example arises if we set $\alpha=40$ and vary β (see Fig. 3). For $\beta=5$ there is a small Eckhaus-like stability region for $r<0.001$; for larger values of r, there remains a single stability region. For larger β, however, the stability region splits into several parts; for example, at $\beta=5.5$ there may be up to five separate intervals of stable traveling waves for a given value of r.

Above we have presented our secondary stability diagrams in the (k,r) plane, for fixed values of α and β. If our interest is in the effects of dispersion on the stability of traveling waves then it is more instructive instead to fix r and present results in either the (k,α) or the (k,β) plane. Our first example is for $r=0.01$ and $\beta=0$ [see Fig. 4(a)]. Given this value of r, the traveling waves exist for $0.9487<k<1.0488$. We expect that if α is small enough then all roll solutions are unstable; this is indeed the case. For larger values of α, a region of stable rolls appears. In Fig. 4(b), we show a second case, where we fix $\alpha=40$ and $r=0.1$, to emphasize that the structure of the stability region may be rather complicated, exhibiting a sensitive parameter dependence.

IV. SECONDARY STABILITY OF TRAVELING WAVES: $\alpha,\beta=O(1)$

In this and the following two sections, we analyze the secondary stability of traveling waves [Eq. (7)]. The most

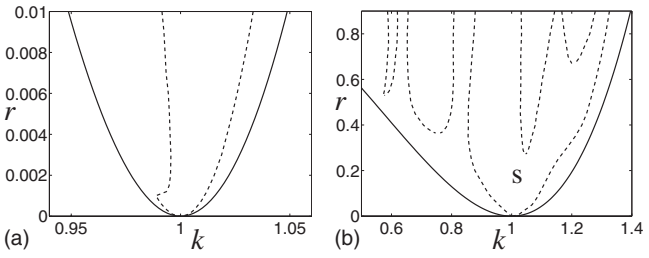

FIG. 3. The secondary stability regions of traveling waves of Eq. (2), calculated numerically for (a) $\beta=5$, (b) $\beta=5.5$, both with $\alpha=40$. Shown are the marginal curve $r=(1-k^2)^2$ (solid line) and the secondary stability boundaries of the traveling waves (dashed line), with stability between the dashed lines. To clarify the regions of stability/instability, the "s" indicates one of the stable regions.

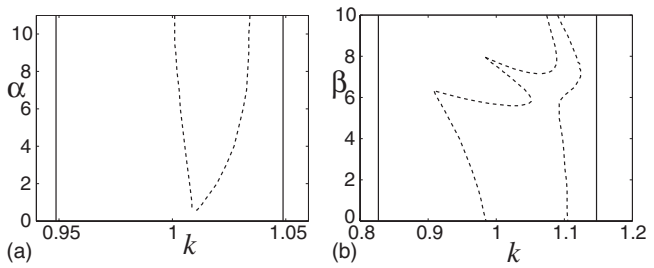

FIG. 4. The secondary stability of traveling waves of Eq. (2) calculated numerically for (a) fixed $\beta=0$ and $r=0.01$ in (k,α) parameter space, (b) fixed $\alpha=40$ and $r=0.1$ in (k,β) parameter space. The marginal curve is represented by the solid lines; traveling waves are stable inside the dashed lines.

straightforward case arises when the dispersion parameters α and β are each $O(1)$. To contrast with later sections, we shall characterize this case as *strong dispersion*. Whereas the nondispersive Nikolaevskiy equation has no *stable* spatially periodic states, Kudryashov and Migita [10] found stable periodic waves in their numerical simulations of the dispersive PDE [Eq. (2)] in this regime.

We begin by introducing the weakly nonlinear expansion

$$u = \epsilon u_1 + \epsilon^2 u_2 + \epsilon^3 u_3 + \cdots, \tag{12}$$

with r given by Eq. (6). Then substitution in Eq. (2) and consideration of successive orders in ϵ leads to the following.

At $O(\epsilon)$, we find that

$$u_1 = A e^{\mathrm{i}(x-c_0 t)} + \text{c.c.},$$

where $c_0=\alpha-\beta$, and where the amplitude A varies slowly in space and in time, in principle depending on the slow variables

$$X = \epsilon x, \quad \tau = \epsilon t, \quad T = \epsilon^2 t.$$

A consideration of the terms proportional to $e^{\mathrm{i}(x-c_0 t)}$ at $O(\epsilon^2)$ then shows that in fact $A=A(\xi,T)$, where

$$\xi = X - (3\alpha - 5\beta)\tau \equiv X - v\tau$$

is a coordinate moving at the group velocity of the waves. Then solving the problem at this order in ϵ yields

$$u_2 = -\frac{\mathrm{i}A^2}{36(1+\mathrm{i}(\alpha-5\beta)/6)} e^{2\mathrm{i}(x-c_0 t)} + \text{c.c.} + f.$$

Here f is a slowly varying function of X, τ, and T, chosen to appear at this order to balance forcing terms appearing at the next order in ϵ.

At $O(\epsilon^3)$, we find, from the respective consideration of the terms in Eq. (2) proportional to $e^{\mathrm{i}(x-c_0 t)}$ and $e^{0\mathrm{i}(x-c_0 t)}$, the amplitude equations

$$\frac{\partial A}{\partial T} = \left[r_2 - \frac{1-\mathrm{i}(\alpha-5\beta)/6}{36+(\alpha-5\beta)^2}|A|^2 \right] A + [4+\mathrm{i}(3\alpha-10\beta)]\frac{\partial^2 A}{\partial \xi^2} - \mathrm{i}fA, \tag{13}$$

$$\frac{\partial f}{\partial \tau} = -\frac{\partial |A|^2}{\partial \xi}. \tag{14}$$

Since $A=A(\xi,T)$, the second amplitude equation suggests taking $f=f(\xi,T)$, in which case Eq. (14) becomes

$$-v\frac{\partial f}{\partial \xi} = -\frac{\partial |A|^2}{\partial \xi},$$

and hence $vf=|A|^2+K(T)$ for some $K(T)$. However, the constraint that the spatial average of u should be zero gives $K(T)=-\langle |A|^2\rangle$, where the angle brackets denote the average in ξ. Thus

$$f = \frac{-\langle |A|^2\rangle + |A|^2}{v} \tag{15}$$

and amplitude Eq. (13) becomes the nonlocal Ginzburg-Landau equation

$$\frac{\partial A}{\partial T} = \left[r_2 - \frac{1-\mathrm{i}(\alpha-5\beta)/6}{36+(\alpha-5\beta)^2}|A|^2 + \mathrm{i}\frac{\langle |A|^2\rangle - |A|^2}{v} \right] A + [4+\mathrm{i}(3\alpha-10\beta)]\frac{\partial^2 A}{\partial \xi^2}. \tag{16}$$

It is worth mentioning that in view of Eq. (15) the present scaling breaks down when v is small; in particular, this is the case when α and β are both small, and this case will be considered in later sections.

It is helpful in analyzing Eq. (16) to put it in canonical form by rescaling all the variables, to give

$$\frac{\partial A}{\partial T} = A + \mathrm{i}d(\langle |A|^2\rangle - |A|^2)A + (1+\mathrm{i}a)\frac{\partial^2 A}{\partial \xi^2} - (1+\mathrm{i}b)|A|^2 A, \tag{17}$$

where

$$a = \frac{3\alpha-10\beta}{4}, \quad b = \frac{5\beta-\alpha}{6}, \quad d = \frac{36+(5\beta-\alpha)^2}{v}.$$

Equations similar to Eq. (17), including a nonlocal nonlinear term have been derived and studied in the context of convection in a rotating annulus [12] and in electrical and magnetic systems [13,14].

Equipped with Eq. (17), we are now in a position to explore the secondary stability of weakly nonlinear spatially periodic solutions of the dispersive Nikolaevskiy equation. Such solutions correspond to plane-wave solutions of Eq. (17), which exist in the form $A=Pe^{\mathrm{i}(\omega T+q\xi)}$, with $P=(1-q^2)^{1/2}$ and $\omega=q^2(b-a)-b$. To study the stability of the plane-wave solution, we write $A=[1+p(\xi,T)]Pe^{\mathrm{i}(\omega T+q\xi)}$, which, after substitution in Eq. (17) and linearization in the perturbation p, yields

$$\frac{\partial p}{\partial T} = (1+\mathrm{i}a)\left(\frac{\partial^2 p}{\partial \xi^2} + 2\mathrm{i}q\frac{\partial p}{\partial \xi} \right) - (1+\mathrm{i}b)P^2(p^*+p) + \mathrm{i}dP^2(\langle p+p^*\rangle - (p+p^*)).$$

Then upon setting $p(\xi,T)=R(T)e^{\mathrm{i}L\xi}+S^*(T)e^{-\mathrm{i}L\xi}$ and equating the coefficients of $e^{\mathrm{i}L\xi}$ and $e^{-\mathrm{i}L\xi}$, we have

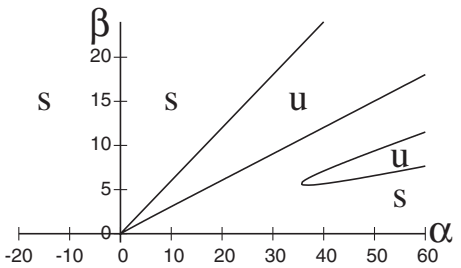

FIG. 5. Diagram showing the sign of $1+a(b+d)$ in $\alpha\beta$ parameter space. Regions with "s" are where $1+a(b+d)>0$ so that a limited band of plane waves is stable, as in (19); a "u" indicates where $1+a(b+d)<0$, and all plane waves are unstable.

$$\frac{dR}{dT} = -(1+ia)L(LR+2qR) - (1+ib)Q^2(R+S) - idQ^2(R+S),$$

$$\frac{dS}{dT} = -(1-ia)L(LS-2qS) - (1-ib)Q^2(R+S) + idQ^2(R+S).$$

Finally, with $R(T)$ and $S(T)$ proportional to $e^{\mu T}$, and expanding the growth rate in powers of the perturbation wave number L, we have the dispersion relation

$$\mu = -2iq(a-b-d)L + L^2P^{-2}(-1-a(b+d)+q^2 \times[3+2(b+d)^2+a(b+d)]) + O(L^3). \quad (18)$$

If we suppose (as is generally the case) that $a \neq b+d$ then it is apparent from Eq. (18) that the solution has a long-wavelength oscillatory instability whenever

$$q^2(3+2(b+d)^2+a(b+d)) > 1+a(b+d).$$

Since $1+a(b+d)<3+a(b+d)+2(b+d)^2$, we see that stability is determined by the following. If $1+a(b+d)>0$ then $3+a(b+d)+2(b+d)^2>0$, and the plane-wave solutions are stable provided

$$0 \le q^2 < q_c^2 \equiv \frac{1+a(b+d)}{3+2(b+d)^2+a(b+d)} < 1. \quad (19)$$

If instead $1+a(b+d)<0$, then all plane waves are unstable. We note that setting $a=b=d=0$ reduces Eq. (17) to a real Ginzburg-Landau equation for A, and our results reduce to the usual Eckhaus instability (with stability for $q^2<1/3$) [15,16].

To apply this result to Eq. (2) it is necessary to indicate the regions in α, β parameter space in which the quantity $1+a(b+d)$ is positive or negative. In Fig. 5, regions denoted by "s" indicate where $1+a(b+d)>0$ so that there are some stable plane waves, as in Eq. (19); those regions denoted by "u" show where $1+a(b+d)<0$, and hence all plane waves are unstable. As discussed in Sec. II, only the region $\beta \ge 0$ need be presented. The existence of a stable region in Fig. 5 is consistent with the numerical results of Sec. III; for example, Fig. 2 shows a stable region when $\alpha=O(1)$ and $\beta=0$.

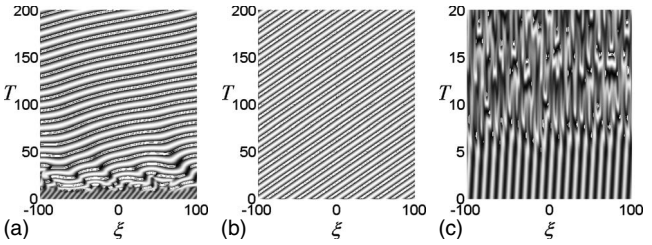

FIG. 6. Numerical simulations of amplitude Eq. (17): in each case the real part of A is plotted as a function of ξ and T. In (a) and (b) $\alpha=10$, whereas in (c) $\alpha=8.4$; in each case $\beta=2.6$. The initial condition in each case is a plane wave, with n wavelengths in the computational box $-32\pi<\xi<32\pi$, plus small-amplitude random noise: (a) $n=28$ (hence $q=0.875$); (b) $n=10$ ($q=0.3125$); and (c) $n=20$ ($q=0.625$).

In Fig. 6, we illustrate the considerations above with some numerical simulations of modified complex Ginzburg-Landau Eq. (17). Our numerical code is pseudospectral, and uses exponential time differencing [17]. In each case the initial condition is a plane wave plus small-amplitude random noise. For the simulations illustrated in Figs. 6(a) and 6(b), $1+a(b+d)>0$. The two plots show the fate of initial conditions in the unstable and stable regions of Fig. 5, respectively. In each case, a stable plane wave is obtained at large T. Figure 6(c) shows the development of instability in the case $1+a(b+d)<0$, where all plane waves are unstable. Here the solution is persistently time dependent.

The analysis above tells us about the secondary stability of traveling-wave solutions of the dispersive Nikolaevskiy equation when $\alpha,\beta=O(1)$, and the results are summarized in Fig. 5. We may think of this analysis as holding for any fixed α and β (not both zero) in the limit as $r \to 0$; thus we expect the lowest part of the secondary stability diagram in (r,k) parameter space to reflect Fig. 5.

However, as indicated earlier, when α and β are both small, the analysis above does not hold and requires reconsideration. We should expect such analysis to break down in this limit because Fig. 5 is inconsistent with the known behavior of the nondispersive Nikolaevskiy equation ($\alpha=\beta=0$) for which all rolls are unstable at onset [3,5]. Thus in Sec. V we consider smaller values of α,β.

V. SECONDARY STABILITY OF TRAVELING WAVES: $\alpha,\beta=O(\epsilon^{3/4})$

It turns out, after some experimentation, that small α and β first lead to a new scaling if we adapt the scaling first used by Tribelsky and Velarde [3] for the nondispersive case and extended by Cox and Matthews [4] to a damped version of the Nikolaevskiy equation. In this scaling the original traveling waves remain $O(\epsilon)$, but the perturbation to the traveling-wave amplitude is $O(\epsilon^{3/2})$ and the large-scale mode is $O(\epsilon^{7/4})$; furthermore, slow spatial and temporal variations of perturbations take place on scales given by $X=\epsilon^{3/4}x$, $T=\epsilon^{3/2}t$, and $\tau=\epsilon^{3/4}t$. (Note that these slow variables are different from those of Sec. IV, but our notation for slow variables is consistent within sections.) To allow the develop-

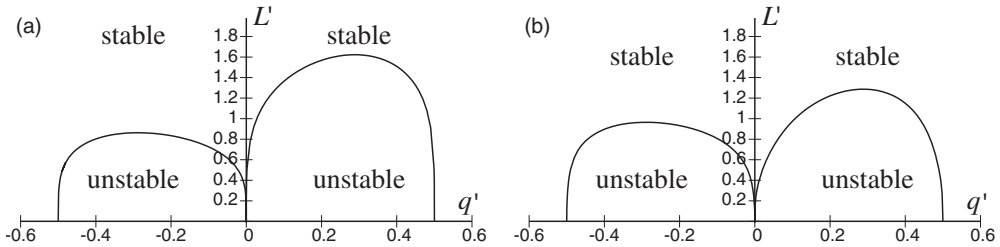

FIG. 7. Predicted secondary stability boundaries of spatially periodic solutions of the Nikolaevskiy equation. (a) Nondispersive case ($v'=0$) and (b) dispersive case ($v'=5$).

ment of consistent amplitude equations for the perturbation we then take

$$\alpha = \epsilon^{3/4}\hat{\alpha}, \quad \beta = \epsilon^{3/4}\hat{\beta}.$$

Applying a weakly nonlinear analysis to Eq. (2) gives

$$u = \epsilon(a_0 + \epsilon^{1/2}a(X,T))e^{iM} + \text{c.c.} + \epsilon^{7/4}f(X,T) + \cdots, \tag{20}$$

where $a_0 = 6\sqrt{r_2 - 4q^2}$,

$$M = (1+\epsilon q)x - \hat{c}\tau - \epsilon^{1/4}\hat{v}qT + \epsilon^{1/4}\psi(X,T),$$

$\hat{c} = \hat{\alpha} - \hat{\beta}$ and $\hat{v} = 3\hat{\alpha} - 5\hat{\beta}$. Here $a(X,T)$ represents disturbances to the amplitude of the pattern, $\psi(X,T)$ represents corresponding disturbances to the phase of the pattern and $f(X,T)$ is a large-scale mode. Substitution of u, as given by Eq. (20), in Eq. (2) requires the consideration of the problem at successive orders in $\epsilon^{1/4}$. After much consequent algebra, we find the (nonlinear) amplitude equations

$$\frac{\partial \psi}{\partial T} = 4\frac{\partial^2 \psi}{\partial X^2} - f - \hat{v}\frac{\partial \psi}{\partial X},$$

$$\frac{\partial f}{\partial T} = \frac{\partial^2 f}{\partial X^2} - 2a_0\frac{\partial a}{\partial X},$$

$$\frac{\partial a}{\partial T} = 4\frac{\partial^2 a}{\partial X^2} - 4a_0\left(\frac{\partial \psi}{\partial X}\right)^2 - 8a_0 q\frac{\partial \psi}{\partial X} - \hat{v}\frac{\partial a}{\partial X}.$$

Note that dispersion is represented in these equations only through the terms $\hat{v}\psi_X$ and $\hat{v}a_X$, representing advection of the pattern envelope with the group velocity $\hat{v}$. Note also that the group velocity of the large-scale mode f is zero, and hence no corresponding term appears in the second of these equations.

The three amplitude equations may be reduced to the single (nonlinear) phase equation

$$\left(\frac{\partial}{\partial T} - 4\frac{\partial^2}{\partial X^2} + \hat{v}\frac{\partial}{\partial X}\right)^2\left(\frac{\partial}{\partial T} - \frac{\partial^2}{\partial X^2}\right)\psi = -16a_0^2\left(\frac{\partial \psi}{\partial X} + q\right)\frac{\partial^2 \psi}{\partial X^2}. \tag{21}$$

Then linearizing this equation and setting $\psi = e^{iLX+\sigma T}$ yields the dispersion relation

$$\sigma^3 + 9\sigma^2L^2 + 24\sigma L^4 - \hat{v}^2\sigma L^2 + 16L^6 - \hat{v}^2L^4 - 16a_0^2qL^2 + i\hat{v}(2\sigma^2L + 10\sigma L^3 + 8L^5) = 0. \tag{22}$$

Before considering this dispersion relation for general L, it is helpful to consider the two limiting cases, of small and large L. First, if L is small, then $\sigma^3 \sim 16a_0^2qL^2$. Thus, to leading order in L, $\sigma = \sigma_{2/3}L^{2/3}$, where $\sigma_{2/3}^3 = 16a_0^2q$; hence all traveling waves are unstable if L is small. On the other hand, if L is large, then we have $\sigma^3 + 9\sigma^2L^2 + 24\sigma L^4 + 16L^6 \approx 0$, and so $\sigma \approx -L^2$ or $-4L^2$ (twice); hence traveling waves are stable to large-L disturbances. In summary, all traveling waves are unstable at onset (provided $a_0^2q \neq 0$; in fact we shall see later that when a_0^2q is suitably small, we shall need to reconsider this conclusion). The rest of the section provides more details of the instability for general values of L.

In order to find the secondary stability boundary for the traveling waves, we set $\sigma = i\Omega$ in dispersion relation (22), where Ω is real. From the real and the imaginary parts, we obtain

$$\Omega^2 - \frac{16}{9}L^4 + \frac{16}{9}a_0^2q + \frac{\hat{v}^2}{9}L^2 + \frac{10}{9}\hat{v}L\Omega = 0,$$

$$\Omega^3 - 24\Omega L^4 + \hat{v}^2\Omega L^2 + 2\hat{v}L\Omega^2 - 8\hat{v}L^5 = 0,$$

and then after eliminating Ω between these two equations we find that this stability boundary is given by

$$16a_0^6q^3 - 2500L^{12} + 2100L^8a_0^2q + 384L^4a_0^4q^2 - 200\hat{v}^2L^{10} - 4\hat{v}^4L^8 - 44\hat{v}^2L^6a_0^2q + \hat{v}^2L^2a_0^4q^2 = 0. \tag{23}$$

We note that in this equation L and $\hat{v}$ appear only as even powers and thus we can restrict our attention to positive L and $\hat{v}$ with no loss of generality. However, both even and odd powers of q occur, so no such economy is possible in considering q (indeed, in the light of [3], we should expect different behaviors for $q>0$ and $q<0$).

For the case of no dispersion, Tribelsky and Velarde [3] showed that, according to the present scaling, there is monotonic instability of the rolls with $q>0$ [with unstable disturbances having $0<L<(a_0^2q)^{1/4}$]. In contrast, oscillatory instability occurs for rolls with $q<0$ [unstable modes having $0<L<(-2a_0^2q/25)^{1/4}$].

It is convenient to present our results for the dispersive case in terms of the rescaled variables $q' = q/r_2^{1/2}$, $L' = L/r_2^{3/8}$, and $v' = \hat{v}/r_2^{3/8}$. Figure 7 illustrates the regions of

stability and instability of the traveling waves, in the cases $v'=0$ and $v'=5$. Note that in the dispersive case all instabilities are oscillatory.

We should view with caution the conclusion above that all traveling waves are unstable because it relies crucially on the assumption that $a_0^2 q$ is not small. The stability analysis above breaks down if q or a_0^2 are small; the true stability properties of corresponding traveling waves will be investigated in Sec. VI.

VI. SECONDARY STABILITY OF TRAVELING WAVES: $\alpha, \beta = O(\epsilon)$

In this section, we investigate the cases of traveling waves with wave number close to $k=1$ or close to the marginal stability boundary, in other words those for which in the previous scaling $a_0^2 q \ll 1$.

A. Traveling waves with close-to-critical wave number

In order to resolve the secondary stability problem for traveling waves with wave number close to $k_c=1$, we set $k=1+\epsilon^2 q$, as was done for the nondispersive case by Tribelsky and Velarde [3]. Then a distinguished balance occurs for $\alpha, \beta = O(\epsilon)$; so we write

$$\alpha = \epsilon\hat{\alpha}, \quad \beta = \epsilon\hat{\beta}.$$

Upon setting $\hat{c}=\hat{\alpha}-\hat{\beta}$, $r=\epsilon^2 r_2$, $\hat{v}=3\hat{\alpha}-5\hat{\beta}$, $X=\epsilon x$, $\tau=\epsilon t$, and $T=\epsilon^2 t$ (the scalings for X and T being as in [3]), we find from Eq. (2) that

$$u = \epsilon(6\sqrt{r_2} + \epsilon^2 a(X,T))e^{iM} + \text{c.c.} + \epsilon^3 f(X,T) + \cdots,$$

where now

$$M = (1+\epsilon^2 q)x - c\tau + \epsilon\left[-\hat{v}q + \tfrac{1}{6}r_2(\hat{\alpha}-5\hat{\beta})\right]T + \epsilon\psi(X,T).$$

The terms in M involving $\hat{\alpha}$ and $\hat{\beta}$ correspond to nonlinear effects of the finite traveling-wave amplitude on the speed of the waves; see Eq. (9).

After much algebra, the relevant (nonlinear) amplitude equations are found to be, at $O(\epsilon^4)$ and $O(\epsilon^5)$,

$$\frac{\partial\psi}{\partial T} = 4\frac{\partial^2\psi}{\partial X^2} - f - \hat{v}\frac{\partial\psi}{\partial X}, \tag{24}$$

$$\frac{\partial f}{\partial T} = \frac{\partial^2 f}{\partial X^2} - 12 r_2^{1/2}\frac{\partial a}{\partial X}, \tag{25}$$

$$\frac{\partial a}{\partial T} = 4\frac{\partial^2 a}{\partial X^2} - 24 r_2^{1/2}\left(\frac{\partial\psi}{\partial X}\right)^2 - \hat{v}\frac{\partial a}{\partial X} - 6 r_2^{1/2}\frac{\partial f}{\partial X} - 2 r_2 a + 6 r_2^{1/2}\left(-8q + \frac{22}{3}r_2 + 12\frac{\partial^2}{\partial X^2} + (10\hat{\beta}-3\hat{\alpha})\frac{\partial}{\partial X}\right)\frac{\partial\psi}{\partial X}. \tag{26}$$

We note that in these equations the influence of dispersion arises not only through the terms involving the group velocity $\hat{v}$ but also through the term $10\hat{\beta}-3\hat{\alpha}$ in the equation for a_T, in contrast to the previous case.

To determine the stability of the traveling waves, these equations are linearized; for solutions proportional to $e^{iLX+\sigma T}$, we find the dispersion relation

$$\sigma^3 + 9\sigma^2 L^2 + 24\sigma L^4 + 16L^6 + 528 r_2^2 L^2 - 576 r_2 q L^2 + 82 r_2 \sigma L^2 - 568 r_2 L^4 + 2 r_2 \sigma^2 - \hat{v}^2\sigma L^2 - L^4\hat{v}^2 + i(2 r_2 \hat{v}\sigma L + 360 r_2\hat{\beta}L^3 + 8\hat{v}L^5 + 10\hat{v}\sigma L^3 + 2\hat{v}\sigma^2 L + 2 r_2 \hat{v} L^3) = 0. \tag{27}$$

As in Sec. V, in the limit of large L, all eigenvalues have negative real part. By contrast, in the limit of small L, if we expand $\sigma=\sigma_1 L+\sigma_2 L^2+\cdots$, then from Eq. (27) we find that σ_1 satisfies

$$r_2\sigma_1^2 - 288 r_2 q + 264 r_2^2 + i r_2 \hat{v}\sigma_1 = 0,$$

whereas σ_2 is determined from

$$\sigma_1^3 + 82 r_2\sigma_1 + 4 r_2\sigma_1\sigma_2 - \hat{v}^2\sigma_1 + 2i(r_2\hat{v}\sigma_2 + \hat{v}\sigma_1^2 + r_2\hat{v} + 180 r_2\hat{\beta}) = 0.$$

The first of these gives

$$\sigma_1 = \frac{1}{2}(-i\hat{v} \pm \sqrt{-\hat{v}^2 + 1152q - 1056 r_2}), \tag{28}$$

and so traveling waves are certainly unstable if their wave number satisfies $q > 11 r_2/12 + \hat{v}^2/1152$. The term $\hat{v}^2/1152$ indicates that these waves become more stable with respect to this instability in the presence of dispersion. If instead $q < 11 r_2/12 + \hat{v}^2/1152$, then σ_1 is purely imaginary, and stability is determined by

$$\sigma_2 = \pm\frac{-72\hat{v}q/r_2 + 171\hat{v}/2 - 180\hat{\beta}}{\sqrt{\hat{v}^2 - 1152q + 1056 r_2}} + \frac{91}{2} - \frac{72}{r_2}q, \tag{29}$$

a consideration of which shows that these waves are made more unstable to the long-wavelength oscillatory instability in the presence of dispersion.

Analysis of the stability boundaries to disturbances of general L is rather involved, and we do not present the details here. Furthermore, the parameter space is large enough to preclude our making general statements; instead we consider some illustrative special cases. To present the conclusions most generally, it is helpful to introduce $q'=q/r_2$, $L'=L/r_2^{1/2}$, $\alpha'=\hat{\alpha}/r_2^{1/2}$, $\beta'=\hat{\beta}/r_2^{1/2}$, and $v'=\hat{v}/r_2^{1/2}$.

Let us begin by considering the special case $\beta'=0$. Figure 8 shows where traveling waves with different values of q' are stable and unstable to perturbations with wave numbers L'; each panel in the figure corresponds to a different choice of α'. In understanding the sequence of transitions in the topology of the various panels, it is helpful to first consider the behavior of the stability boundaries for small α' (and hence small v'), in particular in the $L'=0$ limit. We have seen above that the right-hand stability curve (labeled R) intersects the q' axis at $q'_+ = 11/12 + v'^2/1152$. For small $\hat{v}$, it follows from Eq. (29) that the left-hand stability curve (labeled T) intersects the q' axis at $q'_- \sim 91/144$

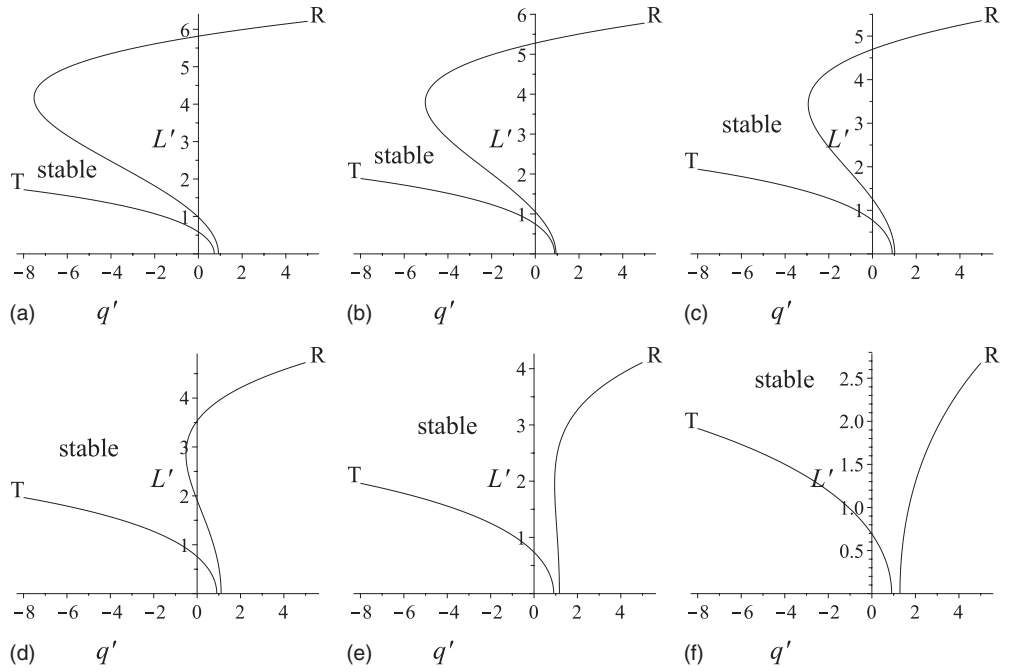

FIG. 8. The stability boundaries for traveling waves according to the amplitude Eqs. (24)–(26), in the special case $\beta'=0$, for different values for α': (a) $\alpha'=1$, (b) $\alpha'=3$, (c) $\alpha'=4$, (d) $\alpha'=5$, (e) $\alpha'=5.7$, and (f) $\alpha'=7$. See the text for more details.

$+5|v'|/26\,568^{1/2}$. Thus as α' is increased from zero, q'_- moves to the right more rapidly than does q'_+. Eventually, at some sufficiently large value of α', $q'_-=q'_+$, and all traveling waves are unstable in the limit $L'=0$. On the other hand, when α' is large, q'_- halts at $q'_-=131/144$. However, q'_+ continues to increase, and this results in the appearance of a small-L' stability region. In fact, for sufficiently large α', some rolls are stable to disturbances for all L'. For $0\leq\alpha'<\alpha'_c$, where $\alpha'_c\approx5.7$, all traveling waves are unstable. For $\alpha'>\alpha'_c$, a stable region appears [see Fig. 8(e)]. Subsequently, for any value of $\alpha'>\alpha'_c$ the stable region becomes more apparent.

This result can be compared with the numerical stability results shown in Fig. 2(a), where $\alpha=1/2$. The stability condition $\alpha'>\alpha'_c\approx5.7$ (where $\alpha'=\alpha/\sqrt{r}$) corresponds to $r<(\alpha/5.7)^2=0.0077$, showing remarkably good agreement with the upper limit of the stable region in Fig. 2(a).

If instead we consider the special case $\alpha'=0$, with $\beta'>0$, we find a broadly similar picture, in that all traveling waves are unstable when β' is small, but some eventually stabilize once β' is sufficiently large. From Fig. 9 it is apparent that the two stability boundaries R and T intersect, coalesce, then lift off from the q' axis as β' is increased. Ultimately they reattach to the q' axis, when $\beta'=\beta'_c$, where $\beta'_c\approx5.06$ as shown in Fig. 9(g). For $\beta'>\beta'_c$, there is a region of stable traveling waves.

Let us now express the results above in a form more illuminating for comparison with our earlier numerical secondary stability calculations (Sec. III). As an example, we set $\hat{\alpha}=1$ and $\hat{\beta}=0$ and consider the limit of small L, looking for regions of stable waves as r_2 is varied.

From Eq. (28), rolls are unstable as long as $q>11r_2/12+\hat{v}^2/1152$. If $q<11r_2/12+\hat{v}^2/1152$, then σ_1 is purely imaginary and hence σ_2 must be considered. From Eq. (29) we have definite instability if $r_2>144q/91$. In addition to these rather blunt conditions, the sign of σ_2 must also be considered in order to determine the stable region. Figure 10 shows the curves $q=11r_2/12+\hat{v}^2/1152$ (solid line), $q=91r_2/144$ (dashed line) and $\sigma_2=0$ (dotted lines). Any region of stability must lie between the solid and dashed lines. After checking carefully the signs of the eigenvalues, we find that the stable region (indicated by the asterisks in the figure) lies between the two dotted lines in the upper and lower parts of the graph, and between the dotted and solid lines for a small range of intermediate values of r_2 (see Fig. 10). Although they appear almost parallel in Fig. 10(a), for large r_2, as in Fig. 10(b), the two sides of the secondary stability region are no longer approximately parallel.

Note the qualitative similarity between the shapes of the stable regions in Figs. 2 and 10.

The question remains of whether or not this stable region extends to indefinitely large values of r_2. To investigate the large-r_2 behavior of the stability region, we consider large r_2 with $q=O(r_2)$, motivated by the observation, from Fig. 10(b), that stable rolls lie in some region between straight lines in (q,r_2) parameter space. In this limit the stability condition from Eq. (28) simplifies to $q<11r_2/12$, while $\sigma_2=91/2-72q/r_2+O(r_2^{-1/2})$. Hence we can conclude that the region of stable waves for small L and large r_2 is

$$91r_2/144<q<11r_2/12. \tag{30}$$

In summary, the results of this section show that when α and β are $O(\epsilon)$, there can be a narrow region of stable traveling waves near $k=1$ and that there is no upper limit on the size of r_2 allowing stable rolls.

For even smaller values of α and β, of order ϵ^2, we have checked that α and β do not appear in the leading-order

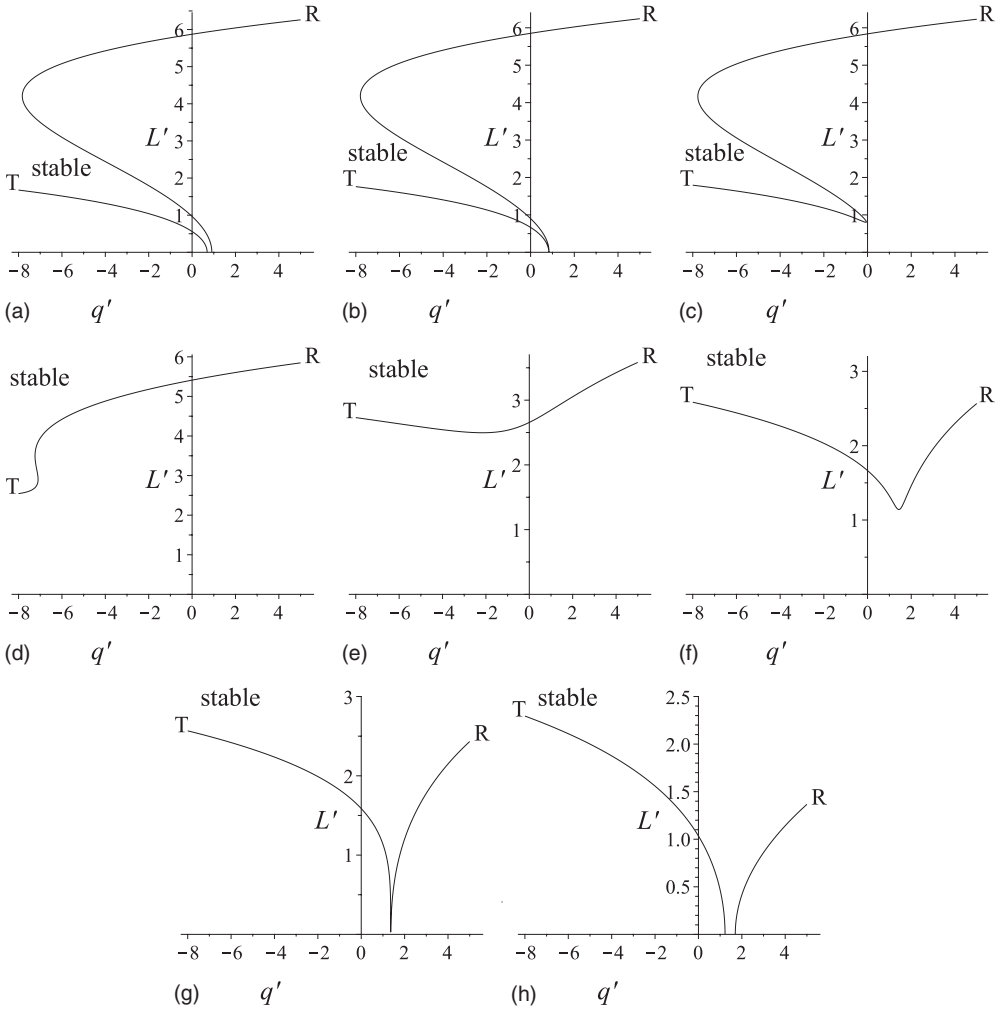

FIG. 9. The stability boundaries for traveling waves according to the amplitude Eqs. (24)–(26), in the special case $\alpha'=0$, for different values for β': (a) $\beta'=0.2$, (b) $\beta'=0.476$, (c) $\beta'=0.6$, (d) $\beta'=2$, (e) $\beta'=4.5$, (f) $\beta'=5$, (g) $\beta'=5.0607$, and (h) $\beta'=6$. See the text for more details.

amplitude equations, so in that case all traveling waves are unstable, as in the nondispersive case.

B. Traveling waves close to the marginal curve

We now turn to the second case in which $a_0^2 q$ may be small: in the region close to the marginal stability curve. Following an analysis similar to that for the dissipative Nikolaevskiy equation [4], we find that, in contrast to the dissipative case (in which a narrow region of stable rolls exists close to the marginal curve [4]), here all traveling waves are unstable near the marginal curve.

VII. NUMERICAL SIMULATIONS OF THE DISPERSIVE NIKOLAEVSKIY EQUATION

To illustrate some of the consequences of the results of the preceding sections, we have carried out numerical simulations of the dispersive Nikolaevskiy equation, using a pseudospectral method, with exponential time stepping [17], of which a small sample are presented here. The initial condition is taken to be a traveling wave with a given wave number k [approximated as a cosine of the amplitude given by Eq. (8)], plus small random noise, and the domain size is $D=100\pi/k$. Figure 11 illustrates, in order, (a) strong, (b)

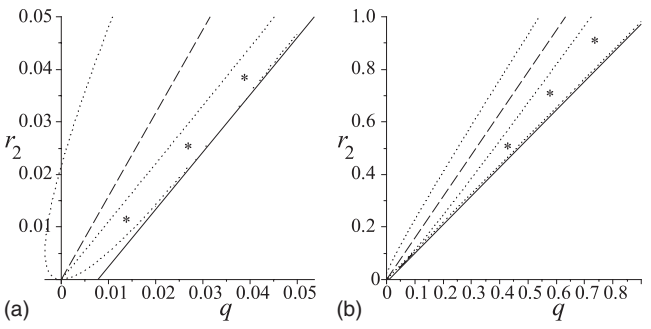

FIG. 10. The region of secondary stability of traveling waves is marked with asterisks; for details refer to the text. The solid line shows where σ_1 is purely imaginary; to the right of this line, the traveling waves are certainly unstable. The dashed line shows where $q=91r_2/144$; to the left of this line, traveling waves are also certainly unstable. The dotted lines show where $\sigma_2=0$.

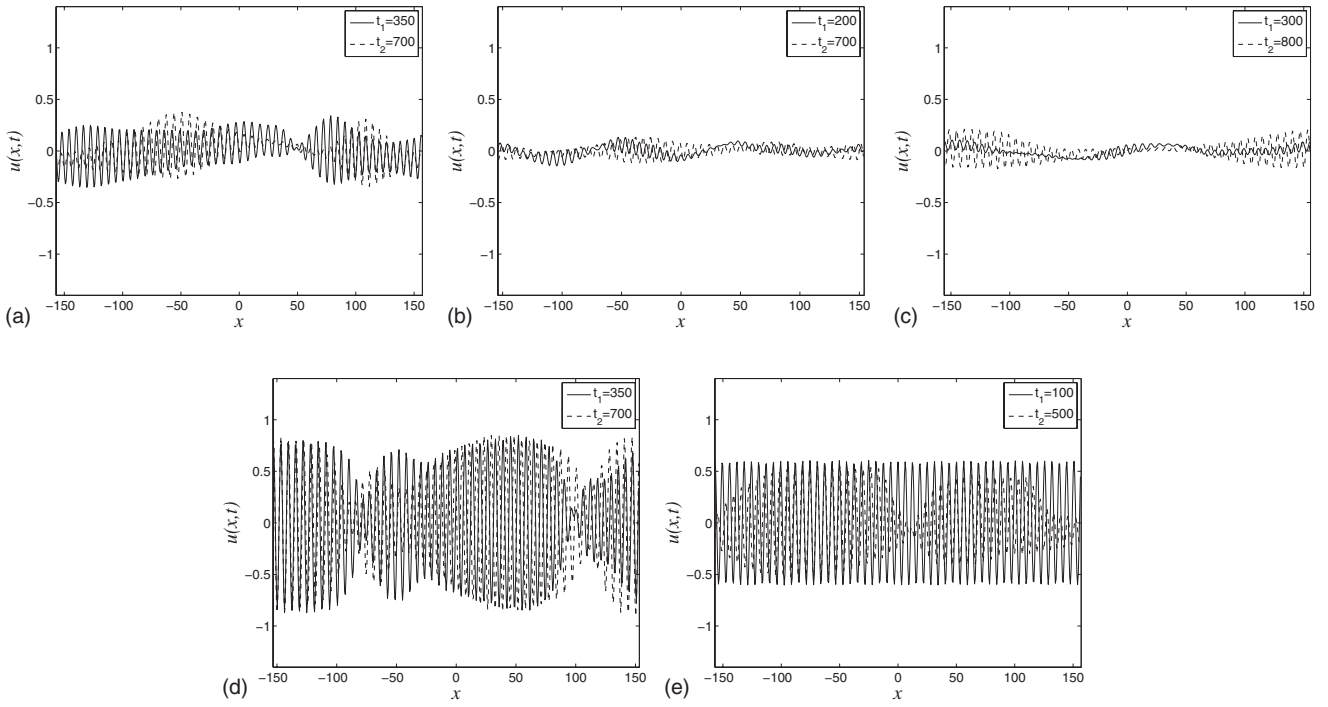

FIG. 11. Snapshots of the numerical solutions of Eq. (2). Parameter values are: (a) $\alpha=2$, $\beta=1$, $r=0.01$, and $k=1$; (b) $\alpha=0.3557$, $\beta=0.1778$, $r=0.01$, and $k=1.02$; (c) $\alpha=0.2$, $\beta=0$, $r=0.01$, and $k=1.0087$; (d) $\alpha=0$, $\beta=0.5$, $r=0.01$, and $k=1.025$; and (e) $\alpha=0.25$, $\beta=0$, $r=0.0025$, and $k=1.00125$. The times of the snapshots are indicated in the insets.

intermediate, and (c)–(e) weak dispersion. The values of α, β, and k are chosen in each case to correspond to traveling waves that are predicted to be unstable by the asymptotic analysis.

Figure 11(a) shows the case of strong dispersion, with $\alpha=2$ and $\beta=1$, and wave number $k=1$ and $r=0.01$. The stability analysis of Eq. (17) predicts that the rolls are unstable, since $\alpha=2$ and $\beta=1$ lie in the unstable region in Fig. 5; the numerical simulation agrees with this asymptotic result.

In Fig. 11(b) an example of intermediate dispersion is simulated, where $\alpha=2\epsilon^{3/4}$ and $\beta=\epsilon^{3/4}$, $r=\epsilon^2$ and $k=1+\epsilon q$, for $q=0.2$ and $\epsilon=0.1$. It is known from the asymptotic results of Sec. V that α and β being $O(\epsilon^{3/4})$ with wave number $k=1+\epsilon q$ will result in unstable traveling-wave solutions, which agrees with the simulation shown in Fig. 11(b).

To show the effects of weak dispersion with wave number $k=1+\epsilon^2 q$ we take $r=0.01$ and $\epsilon=0.1$. Figure 11(c) shows the case $\alpha=2\epsilon$, $\beta=0$, and $q=0.87$, while in Fig. 11(d) the parameter values are $\alpha=0$, $\beta=5\epsilon$, $q=2.5$. Rolls should in each case be unstable, according to the analysis of Sec. VI A, and this is confirmed by the numerical simulations.

Figure 11(e) represents weak dispersion, with $\alpha=\epsilon$ and $\beta=0$. The wave number is $k=1+\epsilon^2 q$ and $r=\epsilon^2 r_2$, for $\epsilon=0.25$, $q=0.02$ with $r_2=0.04$. These values of r_2 and q lie in the unstable region given in Fig. 10, and the simulations support this prediction of instability.

VIII. CONCLUSIONS

We have examined the stability of spatially periodic solutions to the dispersive Nikolaevskiy equation, which is the original model introduced by Nikolaevskiy [1] for seismic waves. The reincorporation of dispersive effects stands in contrast to most studies subsequent to Nikolaevskiy's paper. We have shown how the instability of *all* spatially periodic solutions at the onset of pattern formation in the more-often treated, nondispersive version is modified by the presence of dispersive terms. Our results have been achieved through both a numerical calculation of the secondary stability boundary for the traveling-wave solutions and an asymptotic treatment of three particular scalings in ϵ for the dispersive terms. The secondary stability diagrams ("Busse balloons") can be rather complicated, and can depend sensitively on the size of the dispersive terms.

Our consideration of the case $\alpha,\beta=O(1)$ can be interpreted as giving information about the bottom of the secondary stability diagram obtained in (k,r) parameter space for fixed α and β. Two cases were found: either all traveling waves are unstable at the bottom of the diagram, or there is a symmetrical, Eckhaus-like region of stable traveling waves, right down to onset at $r=0$ (although the width of the region of stable rolls does not stand in the usual Eckhaus ratio to the width of the existence region of rolls).

The separate analysis for smaller values of α,β can be interpreted as shedding light on the upper parts of the fixed-α,β stability diagram in k,r parameter space. We have shown that for small α,β, a narrow region of stable waves may exist near $k=1$. However, beyond the range of validity of the asymptotic analysis, the numerical stability results show the complicated nature of the secondary stability boundaries, so we are unable to draw any significant general conclusions about the form of the secondary stability diagram, limiting ourselves to some specific examples. Things

are further complicated by the fact that rolls predicted to be stable by the asymptotics may in fact turn out to be unstable when the full numerical calculation is performed, since the asymptotics concerns only long-wavelength instabilities, and other, short-wavelength instabilities may turn out to be present.

In this paper, we have said little about the behavior of time-dependent solutions of the dispersive Nikolaevskiy equation. However, it appears from our numerical simulations that when all waves are unstable, chaotic states are found that have a similar behavior to that found in the nondispersive Nikolaevskiy equation [5–7].

[1] V. N. Nikolaevskiy, in *Recent Advances in Engineering Science*, Lecture Notes in Engineering No. 39, edited by S. L. Koh and C. G. Speziale (Springer-Verlag, Berlin, 1989), pp. 210–221.
[2] H. Fujisaka and T. Yamada, Prog. Theor. Phys. **106**, 315 (2001).
[3] M. I. Tribelsky and M. G. Velarde, Phys. Rev. E **54**, 4973 (1996).
[4] S. M. Cox and P. C. Matthews, Phys. Rev. E **76**, 056202 (2007).
[5] P. C. Matthews and S. M. Cox, Phys. Rev. E **62**, R1473 (2000).
[6] M. I. Tribelsky and K. Tsuboi, Phys. Rev. Lett. **76**, 1631 (1996).
[7] H. Sakaguchi and D. Tanaka, Phys. Rev. E **76**, 025201(R) (2007).
[8] R. W. Wittenberg and K.-F. Poon, Phys. Rev. E **79**, 056225 (2009).
[9] B. A. Malomed, Phys. Rev. A **45**, 1009 (1992).
[10] N. A. Kudryashov and A. V. Migita, Fluid Dyn. **42**, 463 (2007).
[11] T. Kawahara, Phys. Rev. Lett. **51**, 381 (1983).
[12] E. Plaut and F. H. Busse, J. Fluid Mech. **464**, 345 (2002).
[13] J. Duan, H. V. Ly, and E. S. Titi, Z. Angew. Math. Phys. **47**, 432 (1996).
[14] F. J. Elmer, Physica D **30**, 321 (1988).
[15] W. Eckhaus, *Studies in Nonlinear Stability Theory*, 7th ed. (Springer-Verlag, Berlin, 1965).
[16] R. Hoyle, *Pattern Formation: An Introduction to Methods* (University Press, Cambridge, 2006).
[17] S. M. Cox and P. C. Matthews, J. Comput. Phys. **176**, 430 (2002).